Surface tension of equilibrium spherical drops in the vapor phase

Yu. K. Tovbin and A. B. Rabinovich*

L. Ya. Karpov Physicochemical Research Institute,
10 ul. Vorontsovo pole, 105064 Moscow, Russian Federation.
E-mail: tovbin@cc.nifhi.ac.ru

The dependence of surface tension of equilibrium spherical drops in the vapor phase on their size at the saturation vapor pressure was studied. The calculation was based on the lattice-gas model in the quasichemical approximation, which takes into account the correlation effects of the nearest interacting molecules. The methods for calculation of the surface tension using a reference surface were considered. The key method is the calculation using an equimolecular reference surface. In the calculation by determining the force moment balance of the transition region, the reference surface is shifted toward the liquid phase of the drop, although the surface tension values are rather similar for both methods. For equilibrium drops, the notion of tension surface was found to be absent. The temperature dependences of the surface tension were studied. The critical sizes of the drops corresponding to the conditions of drop stability as a condensed phase were elucidated.

Key words: spherical drops, width of interfacial layer, equimolecular surface, surface tension, lattice-gas model, quasichemical approximation.

The problem of calculation of the thermodynamic properties of drops remained topical for a long period of time. These properties are needed both to determine thermodynamic characteristics of vapor—liquid systems and to describe the dynamics of new phase formation processes.[1—4] Transition to molecular models is rather slow.[5—10] Due to severe computation problems related to the use of integral equations,[5—8] the characteristics of drops[15] are often calculated using the van der Waals theory of capillarity,[7,9,10] the density functional theory,[11—14] and molecular dynamics. The approach based on the lattice-gas model (LGM)[16—19] was used not only to calculate the planar vapor—liquid interfaces[6,7,20—23] but also to describe curved surfaces.[24,25]

Using the molecular theory,[16,17] the possibilities of description of the state of drops were extended: apart from metastable drops, it became possible to study equilibrium drops, which exist at a saturation vapor pressure. This work reports the first calculation of the surface tension (σ) of equilibrium drops. Comparative analysis of the key methods of determination of the σ value for equilibrium drops, which are similar to the calculation methods of σ in the thermodynamics and continuum mechanics for metastable drops, was carried out. The results of these calculations in terms of the density functional theory were considered previously.[26]

We will restrict ourselves to qualitative description of the molecular distribution and will take into account the interactions of only the nearest neighbors in the quasichemical approximation.

Model

A drop formed by molecules with diameter λ will be modeled by a system comprising spherical monolayers surrounding the drop center. Each monolayer has width λ equal to the molecular diameter and consists of elementary cells or units with the volume $v_0 = \lambda^3$. As the drop radius R, we take the radius of the sphere inside which the drop has homogeneous properties. The transition or interfacial region consists of κ spherical monolayers including one liquid monolayer and one vapor monolayer (Fig. 1). Let us enumerate the spherical monolayers of the transition region q ($1 \le q \le \kappa$) from the liquid ($q = 1$) to the vapor ($q = \kappa$). We will assume that all units within one monolayer have the same properties and will ascribe the type designated by the number of this monolayer q to all of them.

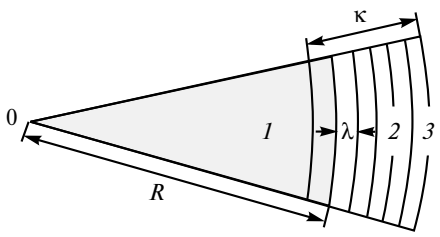

Fig. 1. Schematic fragment of a drop with radius R whose inner part (*1*) is filled with the liquid and the outer part (*3*) is filled with vapor. The liquid to vapor transition region (*2*) consists of κ spherical monolayers of width λ including one liquid monolayer and one vapor phase monolayer.

Published in Russian in *Izvestiya Akademii Nauk. Seriya Khimicheskaya,* No. 4, pp. 663—671, April, 2010.

The considered system is an analog of equilibrium two-phase system at the given temperature T. All sizes in the system (drop radius, width of the transition region, *etc.*) will be measured in the λ units.

For large drops, deviations of the structural fragments from the strictly regular rectangular lattice are minor.[16,17] For the spherical layers of a drop, one can retain the lay-by-layer way of description of the number of bonds $z_{q,p}(R)$ formed by a molecule located in monolayer q with the nearest neighboring molecules located in the same monolayer, $p = q$, or in the neighboring monolayers, $p = q\pm1$ and $\sum_{p=q-1}^{q+1} z_{q,p}(R) = z$ (z is the lattice coordination number). For a regular rectangular lattice, the numbers $z_{q,p}$ are constant. For example, for $z = 6$, we have $z_{q,q\pm1} = 1$, $z_{q,q} = 4$.

The number of units in a spherical monolayer at $R > 5$ is to a high accuracy equal to $N_q(R) \approx 4\pi r^2$, $r = R + q - 1$. For every type of units q, we will define $F_q = N_q(R)/N$, *i.e.*, the fraction of units of the given type in the transition region, where $N = \sum_{q=1}^{\kappa} N_q(R)$ is the number of all units in the transition region.

With allowance for the balance condition of bonds between neighboring layers $N_q(R)z_{q,q+1}(R) = N_{q+1}(R)z_{q+1,q}(R)$, the numbers $z_{q,p}(R)$ will be specified by the relations

$$z_{q,q-1}(R) = (1 - \alpha/r)z_{q,q-1},$$

$$z_{q,q+1}(R) = [1 + (2 - \alpha)/r + (1 - \alpha)/r^2]z_{q,q+1}, \quad (1)$$

$$z_{q,q}(R) = z_{q,q} - 2[(1 - \alpha)/R]\{1 + [1/(2R)]\}z_{qq\pm1}. \quad (2)$$

Equations (1) and (2) are interpreted as approximation expressions for two limiting cases: $\alpha = 0$ and $\alpha = 1$.[17]

The transition region can be regarded as analog of an equilibrium two-phase system at a given temperature T. Since no external forces act on the drop, then according to the LGM theory,[18] which takes account of the inhomogeneity of filling of the system units and interactions between the nearest molecules, one gets the following set of equations[17]

$$P_q = [\theta_q/(1 - \theta_q)]\Lambda_q(R), \ 1 \le q \le \kappa, \quad (3)$$

which relate the local isothermal pressure P_q to the local densities of the fluid θ_q in the monolayers of the liquid—vapor transition region. The nonideality function of the system $\Lambda_q(R)$ in Eq. (3) is specified by the formula

$$\Lambda_q(R) = \prod_{p=q-1}^{q+1} (S_{q,p})^{z_{q,p}(R)},$$

where $S_{q,p} = 1 + xt_{q,p}$, $t_{q,p}$ is the conditional probability that a molecule in monolayer p is located near a unit of monolayer q,[18] $x = \exp(-\beta\varepsilon_{AA})$, ε_{AA} is a parameter of lateral interaction of the nearest molecules; $\beta = (k_B T)^{-1}$, k_B is the Boltzmann constant. The average density of the transition region is defined as $\theta = \sum_{q=1}^{\kappa} F_q\theta_q$.

Free energy of the system. Free energy related to the transition region is written in the quasichemical approximation[27] in the following form:

$$E = \sum_{q=1}^{\kappa} \sum_{i=A,V} F_q M_q^i \theta_q^i, \quad (4)$$

$$M_q^i = \Delta_{i,A}\varepsilon_{AA} \sum_p z_{q,p}(R) t_{q,p}^{AA} - \beta^{-1}(\ln\theta_q^i + 0.5\sum_p z_{q,p}(R)\ln[\theta_{q,p}^{ii}/(\theta_q^i\theta_p^i)]. \quad (5)$$

Here the index A implies an occupied unit, and the index V means a vacant unit; $\theta_q^A = \theta_q$, $\theta_q^V = 1 - \theta_q^A$, $\theta_{q,p}^{ij}$ are the probabilities that a pair of particles i and j are located in the neighboring units in monolayers q and p, Δ_{iA} is the Kronecker symbol (this contribution is absent for vacancies). Expression (4) for the free energy is normalized to one unit of the system.

Determination of the width of the transition region

For the sake of simplicity, consider the system with the coordination number $z = 6$. For a specified temperature T, according to the Maxwell rule,[18,19] determine the saturation vapor pressure $P_s(T)$ and the densities of the coexisting liquid and vapor phases, $\theta^{(L)}$ and $\theta^{(V)}$, respectively, in the bulk phase. Substitute $P_q \equiv P_s(T)$ into the set of equations (3). This gives the so-called equilibrium set of equations. The smallest κ value at which a solution θ_q ($1 \le q \le \kappa$) to the considered set exists will be taken as the width of the transition region; this will be called the density profile of the transition region. The transition region profile changes monotonically with increase in q from $\theta_1 = \theta^{(L)}$ to $\theta_\kappa = \theta^{(V)}$. For a specified drop radius R, the found value will be designated $\kappa(R)$. As shown by calculations, the width of the interfacial region of the drop $\kappa(R)$ does not exceed the width κ of a planar interface at the same temperature.

The solution of the equilibrium set of equations (3) does not depend on the way of determining the surface tension σ. This allows one to compare the existing thermodynamic definitions of the surface tension as applied to equilibrium drops using one and the same concentration profile.

In metastable drops, pressure jump occurs at the separating reference surface. The position of this surface affects the surface tension and the pattern of the concentration profile.[16]

The surface tension of the drop and the dividing surfaces

The spherical monolayers of the transition region can be regarded as spherical surfaces with the curvature radius determined by the monolayer number: $r = R + q - 1$. The

number of the monolayer determining the tension surface will be designated by ρ_r.

The following methods for determining the position of the reference surface exist in thermodynamics:[1—7] 1) equimolecular method; 2) method based on the use of tension surface; 3) method that implies that the moment of forces in the transition region is equal to zero.[6]

These methods are considered below.

1. The equimoleculear surface is defined based on the lack of excessive adsorption of the substance, *i.e.*, $\rho_r = \rho_e$ is found by solving the equation

$$\sum_{q=1}^{\rho_e} F_q(\theta_1 - \theta_q) = \sum_{q=\rho_e+1}^{\kappa} F_q(\theta_q - \theta_\kappa). \quad (6)$$

2. The tension surface is determined by the ρ_r value at which σ is maximum on variation of ρ_r within the interfacial region, $1 \le \rho_r \le \kappa$. This maximum is designated by σ_m and, hence, $\rho_r = \rho_m$. The tension surface is constructed using the tangential component of the pressure tensor.[6—8]

3. The surface where the moment of forces relative to the ρ_s plane is equal to zero is introduced for the tangential component of the local pressures.[6—8] The position of the dividing surface ρ_s is found by solving the equation

$$\sum_{q=1}^{\rho_s} r_q[M_q^V(T) - \mu_1](r_q - r_1) = \sum_{q=\rho_s+1}^{\kappa} [M_q^V(T) - \mu_\kappa](r_\kappa - r_q), \quad (7)$$

where $r_q = R + q - 1$ и $r_s = R + \rho_s - 1$.

The surface tension σ for a fixed sphere radius is determined based on the excess of the Helmholtz free energy in the transition region. The σ value can be expressed through average local pressures and the tangential pressure components M_q^V in the layers q, which are represented in the LGM by local expansion pressures.[17] For the dividing surface positions ρ_e and ρ_m, the surface tension σ is found from the formula

$$\sigma = (1/F_{\rho_r})[\sum_{1 \le q \le \rho_r} F_q(M_q^V - \mu_1) + \sum_{\rho_r \le q \le \kappa} F_q(M_q^V - \mu_\kappa)]. \quad (8)$$

Here the chemical potential

$$\mu_q = \beta^{-1}\{\ln\theta_q^V + z\ln[\theta_{qq}^{VV}/(\theta_q^V)^2]\}$$

is found on the basis of M_q^V at $\theta_p = \theta_q$, the layer number ρ_r determining the position of the reference surface. The layers with $q \le \rho_r$ have higher density, and μ_1 is the chemical potential of the liquid phase; for $q > \rho_r$, the layers have low density, and μ_κ is the chemical potential of the vapor phase.

For the dividing surface ρ_s corresponding to the condition of zero moment of forces, the surface tension σ_s is found from the equation

$$\sigma_s = \frac{1}{r_s}\left[\sum_{q \le r_s} r_q(M_q^{(T)V} - \mu_1) + \sum_{q > r_s} r_q(M_q^{(T)V} - \mu_\kappa)\right]. \quad (9)$$

Previously,[16] for calculation of the surface tension, the purely thermodynamic definition of σ through average local pressure M_q^V was used. In this work we employ the traditional definitions used in mechanics of the surface tension through the tangential component of the pressure tensor. Let $M_q^{(T)V}$ and $M_q^{(N)V}$ be the tangential and normal components of the pressure tensor, which are related to the average local pressure M_q^V value by the expression $M_q^V = (2M_q^{(T)V} + M_q^{(N)V})/3$.

The equilibrium drops are characterized by the equality condition of the chemical potentials ($\mu_\kappa = \mu_1 = \pi(T)$) inside the drops and in the vapor phase at the saturation vapor pressure $P_0(T)$ and given temperature T. This means that the internal pressure values in the vapor and the liquid coincide being equal to $\pi(T)$; therefore, expression (8) for thermodynamic definition of the surface tension[6,16,27] can be written in the form

$$\sigma = \sum_{q=1}^{\kappa} F_q[M_q^V - \pi(T)]/F_{p_s}. \quad (10)$$

The imposing additional condition of equality of the chemical potentials of molecules in the interfacial region means that the normal components of local pressures are equal in all layers of the interfacial region of equilibrium drops, *i.e.*, $M_q^{(N)V} = M_1^V = M_\kappa^V = \pi(T)$. From this it follows that $M_q^{(T)V} = (3M_q^V - M_q^{(N)V})/2$, therefore

$$\sigma = \sum_{q=1}^{\kappa} F_q(M_q^{(T)V} - M_q^{(N)V})/F_{p_s} = (3/2)\sum_{q=1}^{\kappa} F_q[M_q^{(T)V} - \pi(T)]/F_{p_s}. \quad (11)$$

The additional account for the mechanical condition of equality of normal components in all layers between the vapor and the liquid gives an expression that differs from the purely thermodynamic definition of surface tension[6,16,17] by a constant factor of 3/2. From this it follows that the dimensionless ratio σ/σ_b (σ_b is the surface tension for a regular rectangular lattice) does not depend on the additional account of the mechanical equilibrium.

Properties of the interfacial region

The molecular models, unlike thermodynamic ones, allow one to calculate the density concentration profile of the interfacial region. A method of determination of the width of the interfacial region $\kappa(R)$ and the density concentration profiles of the transition region is described above. The radius of the liquid part of the drop R is an additional state parameter of the drop—vapor system. The κ value depends on the radius R and the temperature.[1—7]

The temperatures are presented in the dimensionless form $\tau = T/T_c$, where T_c is the critical temperature in the bulk phase (defined as the temperature at which two-phase regions (indicating separation into layers) disappear.

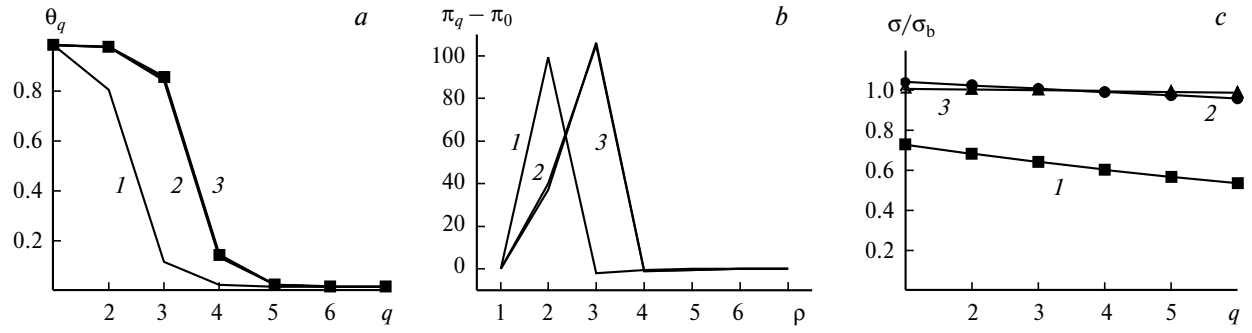

Fig. 2. Effect of the number of the layer q in the interfacial region on the local concentration θ_q (*a*), the $\pi_q - \pi_0$ value (*b*), and the surface tension σ/σ_b (*c*) for drops with size $R = 30$ (*1*), 120 (*2*), 480 (*3*) for $\tau = 0.55$. Here and below, the drop radii (R) were expressed in the lattice structure parameter values λ related to the Lennard-Jones potential parameter ε as $\lambda = 1.12\varepsilon$.

In addition, for the simplicity of designations, we will use π_q instead of M_q^V and π_0 instead of $\pi(T)$.

Figures 2 and 3 show the curves that demonstrate the effect of the drop radius and temperature on the properties of the interfacial region. A comparison of Figs 2, *a* and 3, *a*, which show the concentration profiles of the interfacial region for three dimensions of drops, shows that an increase in the temperature results in increase in the width of the interfacial region. At low temperature ($\tau = 0.55$, see Fig. 2, *a*), the profiles for $R = 120$ (*2*) and 480 (*3*) almost coincide with the bulk profile, whereas at high temperature ($\tau = 0.82$, see Fig. 3, *a*), the profile even for $R = 480$ (*3*) differs from the bulk profile.

Figures 2, *b* and 3, *b* present the local $\pi_q - \pi_0$ values used in relations (8) and (11) to calculate the surface tension. Their distribution over q determines the final σ values. These values are distributed in different ways in the transition region for different R. With increase in temperature and, hence, increase in the width of the interfacial region, their maximum values sharply decrease and the curves become smoother. The $\pi_q - \pi_0$ values starting from zero sharply increase and after reaching a maximum, decrease almost equally sharply to a negative value, and then slowly increase to zero. In addition, since it follows from relation (7) that $\rho_s < \min_{\pi_q < \pi_0} q$, then ρ_s are shifted toward the drop liquid phase: $\rho_s \leq 3$.

The $\sigma(q)$ values (see Figs 2, *c* and 3, *c*) decrease monotonically with an increase in the layer number q ($1 \leq q \leq \kappa$), as the monolayer q determines the position of the reference surface p_r, the denominator F_{pr} in relation (10) increases with increase in q, while the numerator remains constant. Hence, the maximum of $\sigma(q)$ is attained for $q = 1$. This leads to the key conclusion: the traditional thermodynamic notion of the tension surface as the reference surface located inside the transition region for which the σ value is maximum is inapplicable to the equilibrium drops. The lack of the tension surface for metastable drops at low temperatures was noted previously.[16] Therefore, below we consider only two ways of calculation of the surface tension: the equimolecular method with the choice of ρ_e from relation (6) and the method based on the condition that the moment of forces is equal to zero with the choice of ρ_s from relation (7).

The pattern of the concentration profile at high temperatures is shown in Fig. 4 for $\tau = 0.96$. It can be seen that near the critical temperature, the position of the concentration profile differs appreciably from the profile in the bulk phase even for $R = 800$.

The position of the equimolecular dividing surface ρ_e is unambiguously determined by the concentration profile. The position of the surface ρ_s at which the moments

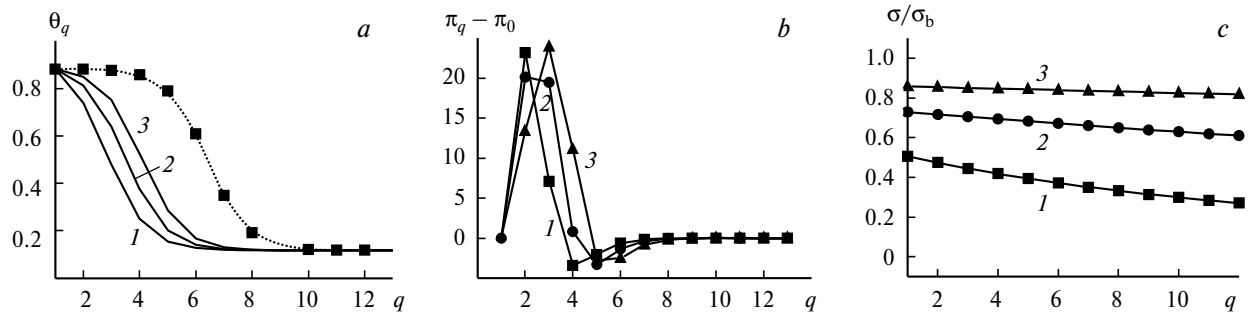

Fig. 3. Effect of the number of the layer q in the interfacial region on the local concentration θ_q (*a*), $\pi_q - \pi_0$ value (*b*), and the surface tension σ/σ_b (*c*) for drops with size $R = 30$ (*1*), 120 (*2*), 480 (*3*) for $\tau = 0.82$. The points in Fig. 3, *a* correspond to a planar interface.

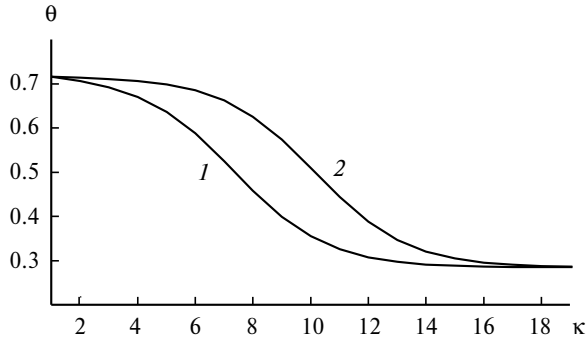

Fig. 4. Dependence of the local filling degrees inside the interfacial region near the critical temperature for $\tau = 0.96$: calculation for drops with the radius $R = 800$ (*1*) and the bulk (*2*).

of forces within the interfacial region become equal depends on the distribution of $\pi_q - \pi_0$ values present in relation (9) over q. The distribution of these values over monolayers q for a planar interface at different temperatures is shown in Fig. 5. As the temperature increases, the $\pi_q - \pi_0$ values rapidly decrease; therefore, for $\tau = 0.96$ these values are shown in the inset on an enlarged scale. It can be seen that the maximum $\pi_q - \pi_0$ values and, hence, the ρ_s values are shifted to low q: $q \le 3$.

Figure 6 shows the temperature dependences of the geometric parameters of the interfacial region for a planar interface: the width of the interfacial region κ (curve *1*) and the positions of reference surfaces ρ_e (curve *2*) and ρ_s (curve *3*). As the temperature increases, both the width of the interfacial region and the number of the layer of the equimolecular dividing surface ρ_e also increase. At a first approximation, $\rho_e = \kappa/2$. At low temperatures, the position of the reference surface ρ_s is close to the ρ_e values but

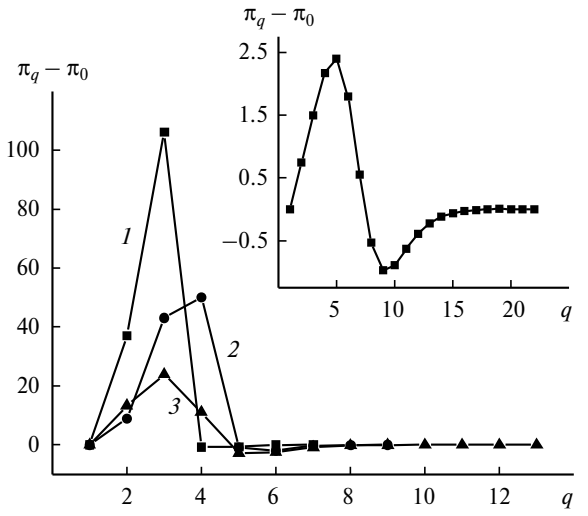

Fig. 5. Dependence of $\pi_q - \pi_0$ on the number of the layer q of the interfacial region of a planar boundary for $\tau = 0.55$ (*1*), 0.68 (*2*), 0.82 (*3*), and 0.96 (in the inset) for an equilibrium drop with the radius $R = 480$.

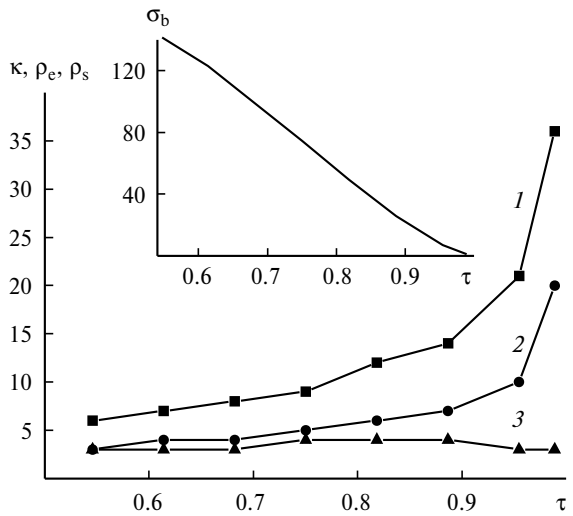

Fig. 6. Dependence of κ (*1*), ρ_e (*2*), ρ_s (*3*) on τ for a planar interface. The inset shows the dependence of surface tension σ_b on τ.

upon increase in the temperature, the ρ_s value remains almost constant.

The inset in Fig. 6 presents the dependence of the surface tension of a planar interface on the temperature. This is consistent with experimental data.[6,7] Over a broad temperature range, this dependence is linear and only in the vicinity of the critical temperature some flexure is observed. The σ value does not depend on the calculation method, because relations (8) and (9) for a planar interface produce one and the same result. These bulk values, designated by σ_b, will be used subsequently to normalize the $\sigma(R)$ values.

In Table 1, the ρ_e and ρ_s values for the same system parameters R and τ as in Fig. 5 are compared. As the temperature increases, the ρ_s value remains almost constant, whereas ρ_e increases.

Figure 7 illustrates the effect of the size of drops on the width of the interfacial region. For different temperatures, the value $\gamma = V_\kappa/V_{drop}$, *i.e.*, the fraction of the volume of the interfacial layer $V_\kappa = \Sigma_{q=2}^{\kappa-1} N_q(R)$ on the full drop volume $V_{drop} = V_{liq} + V_\kappa$, is presented. Here $V_{liq} = 4\pi R^3/3$ is the volume of the liquid part of the drop. As the drop

Table 1. Values ρ_e and ρ_s for drops with the radius $R = 30$ (I), 120 (II), and 480 (III) at the same τ values as in Fig. 5

τ	ρ_c			ρ_s		
	I	II	III	I	II	III
0.55	3	4	4	2	3	3
0.68	3	3	4	2	2	3
0.82	4	4	5	2	2	2
0.96	7	8	8	2	2	2

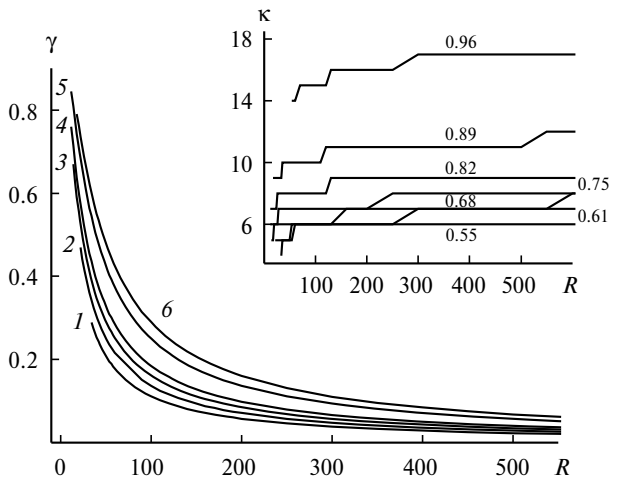

Fig. 7. Dependence of $\gamma = V_\kappa/V_{drop}$ on the drop size R for $\tau = 0.55$ (*1*), 0.61 (*2*), 0.68 (*3*), 0.75 (*4*), 0.82 (*5*), and 0.89 (*6*) at $\alpha = 0.5$. The inset shows the dependence of the number of layers of the transition region κ on the drop radius R; the reduced temperature τ values are indicated in the curves.

size increases, the fraction of the interfacial region in the total volume of the drop sharply decreases.

As the temperature increases, the width of the interfacial region κ, and, hence, the value $\gamma = V_\kappa/V_{drop}$ increase (see the inset in Fig. 7). At $R = 500$, the V_κ value is 3.5% of the total volume of the drop for $\tau = 0.62$ and 6% of the total volume of the drop for $\tau = 0.82$. In the case of small drop sizes, the fraction of the interfacial layer in the total drop volume sharply increases. Near $R = 50$ this fraction reaches 40—50% and in the case of $R = 10$, the interfacial region predominates in the total drop volume.

Figure 8 shows the range of variation of ρ_e for drops with a radius from 8 to 10^3 depending on temperature. The calculation was carried out for seven R values (with a nearly constant increment on a logarithmic scale). It can be seen that the scatter of ρ_e values is only about two monolayers.

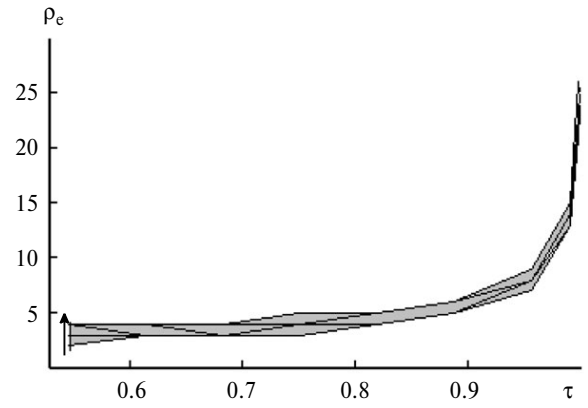

Fig. 8. Ranges for ρ_e variation for drops with the size $R = 8$—1000 *vs.* the reduced temperature τ.

The behavior of curves in Fig. 8 coincides with the behavior of the ρ_e curve in Fig. 6 plotted for a planar lattice.

Dependence of the surface tension on the drop radius

Figure 9 depicts the calculated dependences of σ on the size of drops for different temperatures normalized to the surface tension of a planar lattice σ/σ_b. The calculation was carried out with the parameter $\alpha = 1/2$. It can be seen that with an increase in the drop radius, $\sigma \to \sigma_b$ monotonically, and for lower temperature ($\tau < 0.75$), surface tension jumps are possible. The possibility of such jumps was postulated earlier.[4] These jumps take place at small radius R values; this brings about the question of commensurability of the transition region width and the size of the molecule. In the traditional thermodynamic constructions, it is assumed that the size of the molecule can be neglected. As the temperature increases, the number of monolayers κ increases and the relative change in κ becomes less significant at larger R.

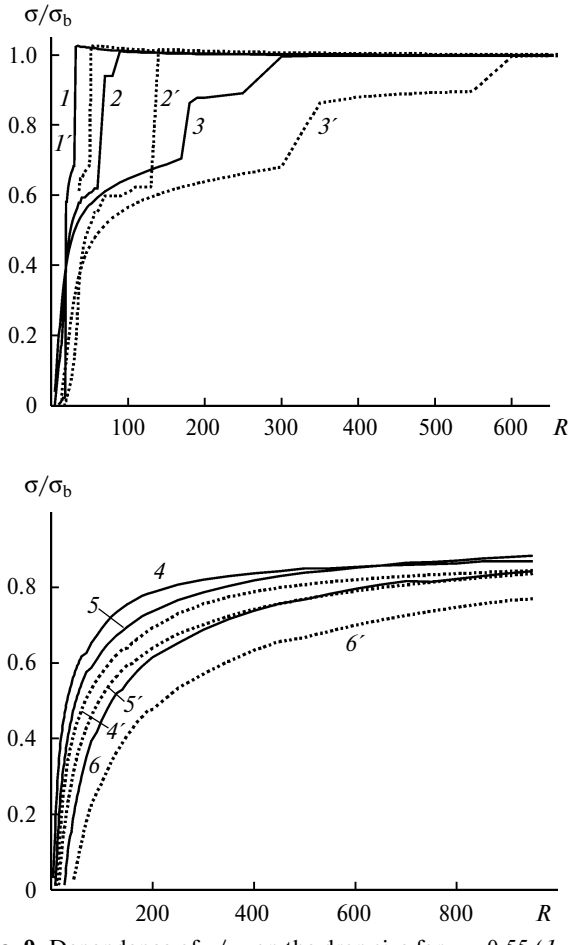

Fig. 9. Dependence of σ/σ_b on the drop size for $\tau = 0.55$ (*1*, *1′*), 0.61 (*2*, *2′*), 0.68 (*3*, *3′*), 0.75 (*4*, *4′*), 0.89 (*5*, *5′*), 0.96 (*6*, *6′*) at $\alpha = 1$ (*1*—*6*) and 0 (1′—6′).

An important role is played by the size range over which the difference between $\sigma(R)$ value in the drop and the bulk σ_b value can be neglected. The region in which the difference between $\sigma(R)$ and the bulk σ_b value is 1% for low temperatures $\tau = 0.55$ and 0.61 starts already at $R \geq 100$. For medium temperatures, the region with this insignificant difference between $\sigma(R)$ and σ_b starts when $R = 600$ for $\tau = 0.68$ and $R = 2500$ for $\tau = 0.75$. At high temperatures a similar difference is observed only at $R \approx 35000$ ($\tau = 0.82$) and $R \approx 10^5$ ($\tau = 0.89$). This is related to the increase in the width of the transition region and convergence of the $\theta^{(L)}$ and $\theta^{(V)}$ values on temperature rise. Previously, this fact was disregarded. To simplify the thermodynamic analysis, bulk value of the surface tension is most often ascribed to relatively small drops.

Different methods for determining the reference surface can give different values of surface tension. Nevertheless, calculations by formulas (8) and (9) for $\alpha = 0$ give rather similar results, which is demonstrated in Fig. 10. It can be seen that both calculation methods give approximately the same σ value.

The temperature dependences of the surface tension of the drops for a number of fixed radius values ranging from 8 to 10^3 are presented in Fig. 11. As above, the values were normalized to the bulk σ_b for every temperature. Curves of two types can be distinguished.

For the first type of curves, for $R \geq 40$ the surface tension is positive starting from low temperature. As temperature increases, σ decreases, although in the intermediate temperature range, the curves may be somewhat non-monotonic. Near the critical temperature, all curves are characterized by negative $\sigma(R)$, which is indicative of instability of drops of this size at high temperatures.

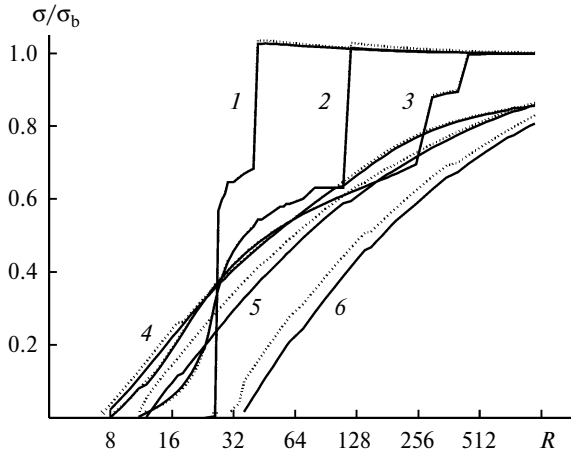

Fig. 10. Dependence of the surface tension calculated by the equimolecular method (continuous lines) and from the equality condition of the moments of forces (dashed line) in the interfacial region for $\tau = 0.55$ (*1*), 0.61 (*2*), 0.68 (*3*), 0.75 (*4*), 0.89 (*5*), 0.96 (*6*) at $\alpha = 0.5$.

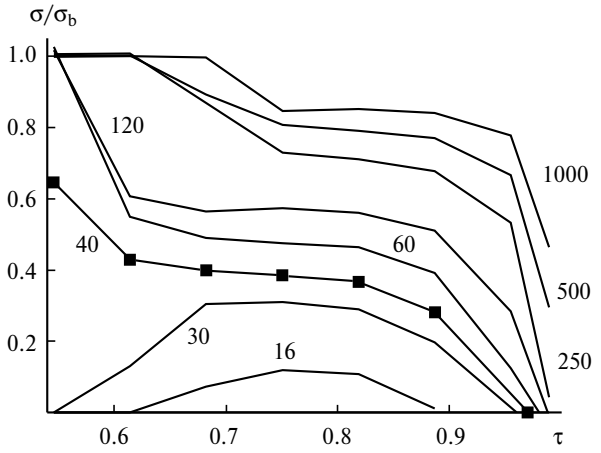

Fig. 11. Dependences of σ/σ_b for drops with sizes R from 16 to 1000 on the reduced temperature τ. The drop radii R are indicated at the curves.

For the second type of curves at $R \leq 30$, σ increases with temperature rise from negative values to a certain maximum and then decreases to negative values, as in the first type of curves. In the case of a positive maximum, for drops of these size range, a temperature region exists in which equilibrium drops are stable. These drops ($R = 16$) cannot exist at low or high temperatures due to negative surface tension. Meanwhile, for $R = 8$, it was found that $\sigma < 0$ and, hence, the drop is unstable at any temperature. Since negative surface tension values imply drop instability, they are not presented in Fig. 11.

The critical sizes of drop formation

Figures 9—11 presented above indicate that there exist solutions to the set of equations (3) for which σ are negative. A surface tension equal to zero implies the loss of stability of the drop as the liquid phase. Actually the condition $\sigma = 0$ means that under these conditions the considered system does not form two phases. This occurs at some critical size of the drops.

It follows from Fig. 11 that the condition $\sigma = 0$ can be attained both by increasing temperature near the critical temperature and by decreasing the drop size. In the former case, the system occurs near large thermal fluctuations and the chosen radii become smaller than the average phase of fluctuations at the given temperature. In the latter case, the "phase" inside the drop becomes unstable due to large fraction of the interfacial region in the total drop volume (see Fig. 7).

Figure 12 shows the temperature dependence of drop size R_0 corresponding to the onset of the formation of the second phase ($\sigma(R_0) = 0$) at three values of parameter α.

The zero α value corresponds to drops at low temperatures and $\alpha = 1$ corresponds to slightly curved monolayers of large drops.[17] It is natural to assume that α depends on

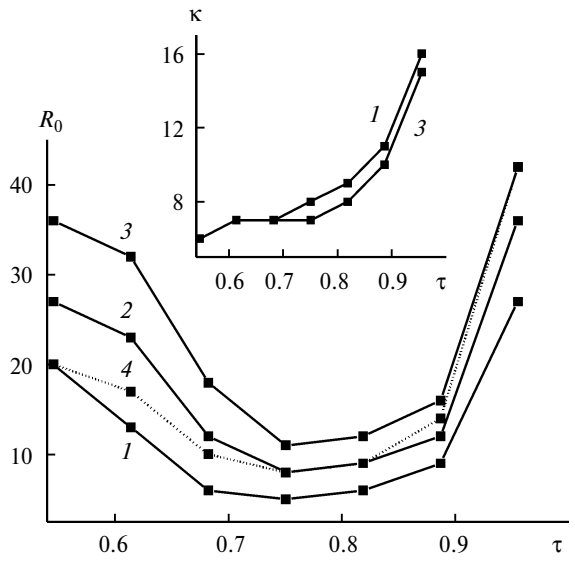

Fig. 12. Drop size corresponding to the onset of formation of the new phase (R_0) at $\alpha = 0$ (*1*), 0.5 (*2*), 1 (*3*) and for linear approximation of $\alpha(T)$ (*4*) *vs.* temperature τ. The inset shows the dependence of the number of layers of the interfacial region κ on τ at $\alpha = 0$ (*1*) и 1 (*3*).

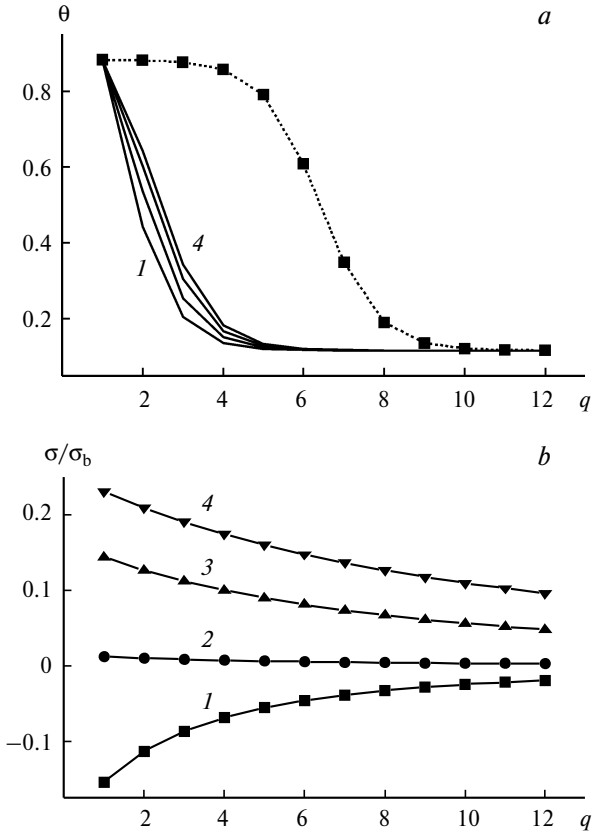

Fig. 13. Concentration profiles (*a*) and normalized surface tensions σ/σ_b (*b*) *vs.* the number of the layer of the interface q for $\tau = 0.82$. The calculations were calculated for drops with the size $R = 6$ (*1*), 10 (*2*), 15 (*3*), and 20 (*4*). The dots in Fig. 13, *a* show the concentration profiles for a planar interface.

temperature and, as a first approximation, to be restricted to the linear dependence on T: $\alpha(\tau) = (\tau - \tau_0)/(1 - \tau_0)$, where $\tau_0 = 0.55$ is the triple point temperature. Curve *4* (see Fig. 12) refers to the given linear approximation of $\alpha(T)$.

For all of the considered α values are characterized by decrease in R_0 at $\tau \le 0.75$ and fast growth of R_0 at $\tau > 0.75$. In addition, an increase in α entails increase in R_0. When $\alpha = 0.5$, they are close to average values between the R_0 values for $\alpha = 0$ and $\alpha = 1$. For linear approximation of $\alpha(T)$, the R_0 values change from the value corresponding to $\alpha = 0$ (at $\tau = 0.55$) to the value corresponding to $\alpha = 1$ (at $\tau \to 1$).

The solution of the set of equations (3) at specified R and T values represent some equilibrium distribution profile of molecules θ_q ($1 \le q \le \kappa$). The existence of this profile does not answer the question whether or not the found solution refers to a stable liquid phase of the drop. This question can be answered considering the sign of the surface tension. If it is positive, the phase is stable, while when it is negative, the phase is unstable.

Figure 13 presents a comparison of the concentration profiles (*a*) and dependences of the normalized surface tensions σ/σ_b (*b*) on the layer number of the interface q at $\tau = 0.82$. The calculations were carried out for small drops. The concentration profiles shown in Fig. 13, *a* have similar form, and the sign of the surface tension cannot be estimated from their pattern. In Fig. 13, *b*, the sign of σ is retained and the surface tension either decreases with increase in the number q if $\sigma > 0$ (curves *2*—*4*) or increases if $\sigma < 0$ (curve *1*).

Nevertheless, the more sharply the profile changes and the lower the width of the interfacial region, the smaller σ.

Analysis of the theoretical equations[16,17] has shown the theoretical possibility of existence of equilibrium drops at equal vapor and liquid pressures. Apparently, vapor phase clusters or associates for highly non-ideal fluids are formed by the same mechanism.[19] Analysis of the states of the system preceding the condensation phase transition where the associates themselves acquire the properties of a new phase with increase in the size is of interest by itself. It is known that only these states correspond to thermodynamic assumptions of the simultaneous equality of the chemical potential of the molecule and the pressure inside the drop and in the bulk vapor phase.[4—7] The existence of critical drop size corresponding to stability conditions of the drop as a condensed phase was demonstrated.

The effect of the surface tension of equilibrium spherical drops in the vapor phase under saturated vapor pressure as a function of their size and the temperature dependences of the surface tension of drops with different size were studied for the first time. Over the whole size range, the $\sigma(R)$ is lower than that for the bulk phase σ_b. It was

found that for equilibrium drops, the notion of "tension surface" is absent. The numerical values of the surface tension for the equimolecular surface and for the surface corresponding to equilibrium to the moments of forces in the transition region are rather close to each other.

The calculations illustrate good prospects for the use of the proposed microscopic approach[16,17] for the description of thermodynamic characteristics of drops. The model can also be used to describe the behavior of small vapor bubbles in the liquid phase. Since the lattice model is widely used in practice,[20—23] this approach allows one to use this model for curved surfaces.

References

1. J. W. Gibbs, *Thermodynamics. Statistical Mechanics*, Nauka, Moscow, 1982, 584 pp. (Russian Translation).
2. M. Volmer, *Kinetik der Phasenbildung*, Verlag von Theodor Steinkopff, Drezden—Leipzig, 1939.
3. Ya. I. Frenkel´, *Kineticheskaya teoriya zhidkostei* [*Kinetic Theory of Liquids*], Izd. AN SSSR, Moscow—Leningrad, 1945, 592 pp. (in Russian).
4. A. I. Rusanov, *Fazovye ravnovesiya i poverkhnostnye yavleniya* [*Phase Equilibria and Surface Phenomena*], Khimiya, Leningrad, 1967, 322 pp. (in Russian).
5. F. P. Buff, J. G. Kirkwood, *J. Chem. Phys.*, 1950, **18**, 991.
6. S. Ono, S. Kondo, *Molecular Theory of Surface Tension in Liquids*, Springer—Verlag, Berlin—Göttingen—Heidelberg, 1960.
7. J. S. Rowlinson, B. Widom, *Molecular Theory of Capillarity*, Clarendon Press, Oxford, 1982.
8. C. A. Croxton, *Liquid State Physics — A Statistical Mechanical Introduction*, Cambridge University Press, Cambridge, 1974.
9. M. Iwamatsu, *J. Phys. Condens. Matter.*, 1994, **6**, L173.
10. V. G. Baidakov, G. Sh. Boltachev, *Zh. Fiz. Khim.*, 1995, **69**, 515 [*Russ. J. Phys. Chem.* (*Engl. Transl.*), 1995, **69**].
11. T. V. Bykov, A. K. Shchekin, *Kolloid. Zh.*, 1999, **61**, 164 [*Colloid. J.* (*Engl. Transl.*), 1999, **61**].
12. T. V. Bykov, A. K. Shchekin, *Neorgan. Materialy*, 1999, **35**, 759 [*Inorg. Mater.* (*Engl. Transl.*), 1999, **35**].
13. T. V. Bykov, X. C. Zeng, *J. Chem. Phys.*, 1999, **111**, 3705.
14. T. V. Bykov, X. C. Zeng, *J. Chem. Phys.*, 1999, **111**, 10602.
15. D. I. Zhukhovitskii, *Kolloid. Zh.*, 2003, **65**, 480 [*Colloid J.* (*Engl. Transl.*), 2003, **65**].
16. Yu. K. Tovbin, A. B. Rabinovich, *Izv. Akad. Nauk, Ser. Khim.*, 2009, 2127 [*Russ. Chem. Bull., Int. Ed.*, 2009, **58**, 2193].
17. Yu. K. Tovbin, *Zh. Fiz. Khim.*, 2010, **84**, 3 [*Russ. J. Phys. Chem.* (*Engl. Transl.*), 2010, **84**, No. 1].
18. Yu. K. Tovbin, *Theory of Physical Chemistry Processes at a Gas—Solid Surface Processes*, CRC Press, Boca Raton, Fl, 1991.
19. T. L. Hill, *Statistical Mechanics. Principles and Selected Applications*, McGraw—Hill Book Comp. Inc., New York, 1956.
20. I. Prigogine, R. Defay, *J. Chim. Phys.*, 1949, **46**, 367.
21. R. Defay, I. Prigogine, A. Bellemans, D. H. Everett, *Surface Tension and Adsorption*, Longmans, Green and Co., London, 1966.
22. A. W. Adamson, *Physical Chemistry of Surfaces*, 3rd ed., Wiley, New York—London—Sydney—Toronto, 1975.
23. N. A. Smirnova, *Molekulyarnye teorii rastvorov* [*Molecular Theories of Solutions*], Khimiya, Leningrad, 1987, 334 pp. (in Russian).
24. C. Appert, V. Pot, S. Zaleski, *Fields Institute Commun.*, 1996, **6**, 1.
25. K. Ebihara, M. Watanabe, *Eur. Phys. J., B*, 2000, **18**, 319.
26. V. Talanquer, D. W. Oxtoby, *J. Chem. Phys.*, 1995, **99**, 2865.
27. Yu. K. Tovbin, *Zh. Fiz. Khim.*, 1992, **74**, 1395 [*Russ. J. Phys. Chem.* (*Engl. Transl.*), 1992, **74**, No. 5].

Received July 30, 2009;
in revised form March 2, 2010